ME 4322 Final Project Report

Team 3: Alex Pappas, Joseph Abinader, Victor Pina

Project Inspiration

Our term project is a continuation of our MQP project which is to build an electric, all terrain wheelchair for Jared Grier. The goal of the project is to design and construct a wheelchair that has all the capabilities to go off road with a minimal footprint so that the wheelchair can still be used indoors. We plan on achieving this by using custom omni wheels and a suspension system on both the front and rear wheels. This coupled with direct drive hub motors on all four wheels should give Jared the desired power to be able to tackle any obstacle in his path.

Critical System Components

The critical aspect of this project is the front suspension for the wheelchair. For the project we are analyzing the force that is applied on the shocks due to the mass of the system. This force is applied at the bottom of the "knuckle" link which is the triangular link that acts as our coupler. The mass distribution for Jared's wheelchair is 1:6 from the front to the rear. The total mass of the chair is 180 lbs, therefore 30 lbs is present in the front and 150 lbs. in the rear. We expect our wheelchair to be lighter, and expect to have a 20 lb normal force on the front wheel. Figures 1 is a visual representation of our suspension system.

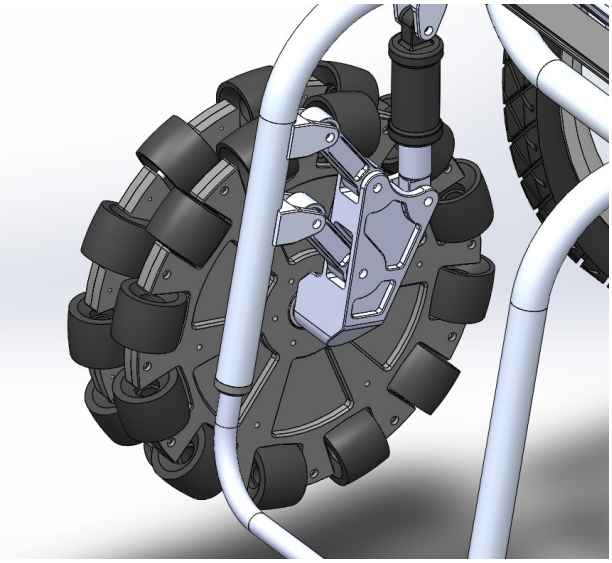

Figure 1: Front Omni Wheel Suspension

Assumptions and Nomenclature

Table 1: Master Nomenclature Table

Symbols	Description
A_y … D_y	Force in the y direction at all given points
A_x … D_x	Force in the x direction at all given points
F_A F_s	Force of the wheelchair and shock respectively
W_1	Rotation of the first link AB
D_i B_i	All damping coefficients for the system
J_1 J_2	Inertias of the first two links AB and CD
M_3	Mass of the knuckle link which acts as our coupler

Table 2: Assumptions Table

Assumptions	Justifications
Wheelchair frame is a rigid body	Frame is composed out of 0.120" structural aluminum, making any elasticity negligible
Applied force from the wheel is applied vertically	The Force applied from the chair is mostly vertical due to the system geometry and how we designed the chair
No wear on the system	It is being newly constructed and built, so it has no wear

Perfect assembly	We believe in our ability and the ability of those we hired to fabricate the chair properly
Small Rotations of the links	V = r ω
Links are rigid bodies	The links are machined out of the same aluminum as the frame
The assembly is constrained to the x-y plane	We have little to no twist in the system since the suspension moves up and down, so we safely say it stays in the x-y plane
Gravity is only accounted for in the knuckle link	The first two links are small and rotate so we ignore their weight, the knuckle moves up and down and is significantly bigger

Free Body Diagram

Our suspension system is what is known as a four bar linkage and the general free body diagram is shown below in Figure 2. The point "E" is where the air suspension is attached to the system and the point F is where the wheel axle is attached. We are trying to determine the force applied to the shocks by the weight of the system in order to determine the optimal pressurization of the shock. Since our design encompasses dual chambered air shocks, we can adjust the amount of pressure inside the shock to adjust how stiff the ride is for Jared. Point "F" is our input and the point "E" is our output. Links CD and AB are revolute joints that are grounded to the frame and link ACEF is the knuckle that connects the wheel axle and the shock absorber. The grounded pivots also have equal and opposite forces to those applied on them by links AB and CD.

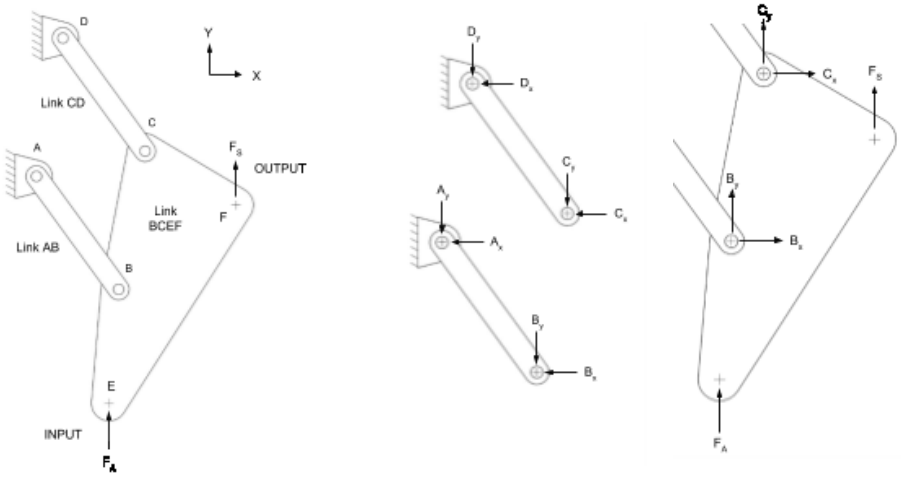

Figure 2: FBD of Entire system and Individual Links

The free body diagrams were used to derive the following static force and moment equations, where g is the grounded shock attachment joint.

$$\sum F_{bcef}\colon\ F_{applied} + F_b + F_c + F_s = \begin{matrix}0\\0\\0\end{matrix} \tag{1.1}$$

$$\sum F_{ab}\colon\ F_b + F_a = \begin{matrix}0\\0\\0\end{matrix} \tag{1.2}$$

$$\sum F_{cd}\colon\ F_c + F_d = \begin{matrix}0\\0\\0\end{matrix} \tag{1.3}$$

$$\sum F_{shock}\colon\ F_s + F_g = \begin{matrix}0\\0\\0\end{matrix} \tag{1.4}$$

$$\sum M_B\ (link\ bcef)\colon\ F_{applied} x\ R_{eb} + F_c\ x\ R_{cb} + F_s\ x\ R_{fb} = \begin{matrix}0\\0\\0\end{matrix} \tag{1.5}$$

$$\sum M_B\ (link\ ab)\colon\ F_b\ x\ R_{ba} = \begin{matrix}0\\0\\0\end{matrix} \tag{1.6}$$

$$\sum M_d\ (link\ cd)\colon\ F_c\ x\ R_{cd} = \begin{matrix}0\\0\\0\end{matrix} \tag{1.7}$$

$$\sum M_g\ (link\ shock, g)\colon\ F_s\ x\ R_{fg} = \begin{matrix}0\\0\\0\end{matrix} \tag{1.8}$$

The position vectors can be solved for by calculating the position of each joint using the following Matlab code.

```
jointA = [0;0];
jointD = [0.59;3.09];
jointG = [4.55;5.85];
% calculate position of joint b
jointB = lba*[cosd(theta); -sind(theta)];
% calculate position of joint c
jointC = [lcd*cosd(theta)+jointD(1); jointD(2)-lcd*sind(theta)];
% calculate position of joint e
alpha = atan2d(jointD(2),jointD(1));
beta = 180 - alpha - theta;
gamma = 360-beta-174;
lae = sqrt(lba^2 + leb^2 - 2*lba*leb*cosd(gamma));
phi = asind((leb*sind(gamma))./lae);
jointE = [lae.*cosd(theta+phi); -lae.*sind(theta+phi)];
% calculate position of joint f
zeta = 360 - (180 - beta) - 70;
ldf = sqrt(lfc^2 + lcd^2 - 2*lfc*lcd*cosd(zeta));
theta2 = theta-asind((lfc*sind(zeta))./ldf);
jointF = [jointD(1) + ldf.*cosd(theta2); jointD(2) - ldf.*sind(theta2)];

% caculate position vectors
rba = -jointB+jointA;
rcb = jointC-jointB;
rcd = -jointC+jointD;
reb = jointE-jointB;
rfc = jointF-jointC;
rfe = jointF-jointE;
rfg = jointF-jointG;

rfb = jointF - jointB;
```

Figure 3: Matlab Code For Joint Positions

The Matlab code assumes opposite links are equal and parallel, as they are in our suspension system, and that joint A is at the origin. The variables l_{ba}, l_{cd}, l_{eb}, and l_{fc} are the link lengths provided by the user. In our case, $l_{ba} = l_{cd} = 3.13$ inches, $l_{eb} = 2.56$ inches, and $l_{fc} = 2.36$ inches. L_{eb}, and l_{fc} are used to find the position of the wheel and shock mounting joints respectively. This code assumes theta is a vector of angles between link ab and the x axis.

By then calculating the link velocities, accelerations, and center of mass equations with the following equations, the dynamic force equations can be solved.

$$V_{cd} = V_{cb} + V_{ba} \quad (2.1)$$

$$V_{input} = V_{eb} + V_{ba} \quad (2.2)$$

$$V_{fg} = V_{fc} + V_{cd} \quad (2.3)$$

Where $V_{nm} = \omega_{nm}\, x\, R_{nm}$.

$$A_{cd} = A_{bcef} + A_{ab} \quad (3.1)$$

$$\alpha_{cd} x\, R_{cd} + \omega_{cd} x(\omega_{cd} x\, R_{cd}) = \alpha_{bcef} x\, R_{cb} + \omega_{bcef} x(\omega_{bcef} x\, R_{cb}) + \alpha_{ab} x\, R_{ab} + \omega_{ab} x(\omega_{ab} x\, R_{ab}) \quad (3.1a)$$

$$A_{fg} = A_{bcef} + A_{cd} \quad (3.2)$$

$$\alpha_{fg} x\, R_{fg} + \omega_{fg} x(\omega_{fg} x\, R_{fg}) = \alpha_{bcef} x\, R_{cb} + \omega_{bcef} x(\omega_{bcef} x\, R_{cb}) + \alpha_{cd} x\, R_{cd} + \omega_{cd} x(\omega_{cd} x\, R_{cd}) \quad (3.2a)$$

$$AM_{ab} = \alpha_{ab} x\, R_{abM} + \omega_{ab} x(\omega_{ab} x\, R_{abM}) \quad (4.1)$$

$$AM_{bcef} = A_{ab} + AM_{bcef} \quad (4.2)$$

$$AM_{bcef} = \alpha_{ab} x\, R_{ab} + \omega_{ab} x(\omega_{ab} x\, R_{ab}) + \alpha_{bcef} x\, R_{bcefM} + \omega_{bcef} x(\omega_{bcef} x\, R_{bcefM}) \quad (4.2a)$$

$$AM_{cd} = \alpha_{cd} x\, R_{cdM} + \omega_{cd} x(\omega_{cd} x\, R_{cdM}) \quad (4.3)$$

$$AM_{fg} = \alpha_{fg} x\, R_{fgM} + \omega_{fg} x(\omega_{fg} x\, R_{fgM}) \quad (4.4)$$

Equations 2.1 through 4.4 show how to solve for all of the necessary link angular velocity and accelerations, and the center of mass accelerations. Note with the center of mass accelerations, R_{nmM} is the position vector from joint n to the center of mass of link nm. By then plugging the solved values into the following equations, the dynamic force at each joint can be calculated.

$$\sum F_{bcef}:\ F_{applied} + F_b + F_c + F_s = M_{bcef} * AM_{bcef} \quad (5.1)$$

$$\sum F_{ab}:\ F_b + F_a = M_{ab} * AM_{ab} \quad (5.2)$$

$$\sum F_{cd}:\ F_c + F_d = M_{cd} * AM_{cd} \quad (5.3)$$

$$\sum F_{shock}:\ F_s + F_g = M_{fg} * AM_{fg} \quad (5.4)$$

$$\sum M_B\ (link\ bcef):\ F_{applied} x\ R_{eb} + F_c\ x\ R_{cb} + F_s\ x\ R_{fb} = I_{bcef} * \alpha_{bcef} \quad (5.5)$$

$$\sum M_B\ (link\ ab):\ F_b\ x\ R_{ba} = I_{ab} * \alpha_{ab} \quad (5.6)$$

$$\sum M_d\ (link\ cd):\ F_c\ x\ R_{cd} = I_{cd} * \alpha_{cd} \quad (5.7)$$

$$\sum M_g\ (link\ shock, g):\ F_s\ x\ R_{fg} = I_{fg} * \alpha_{fg} \quad (5.8)$$

All mass and inertia values necessary were found using the Solidworks model of the suspension system and inserted in Table 3.

Table 3: Inertia and Mass values for All Components

Inertia (lb*in^2)	Mass (lb)
Link DC: 0.38	0.23
Link AB: 0.38	0.23
Shock: 0.98	0.26
Knuckle: 6.6	Knuckle: 1.82

Dynamic Response and Performance

Performing the dynamic analysis over the entire range of our suspension system assuming a 20lb vertical input at joint E resulted in the force response seen in Figure 4.

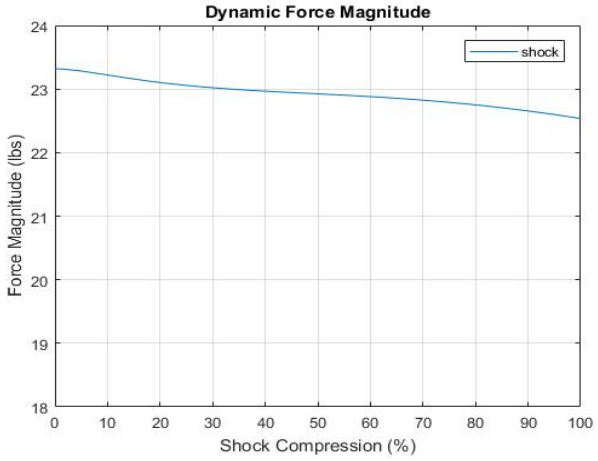

Figure 4: Force vs Shock Compression

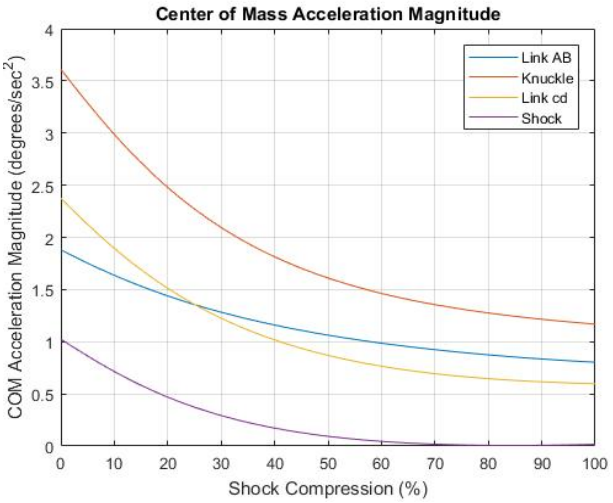

Figure 5: COM Acceleration vs Shock Compression

This type of response is ideal since the shock we are using has a linear response. As the force applied to the shock is shown to be roughly linear, the shock should compress smoothly over its entire range. Figure 5 shows the joints will accelerate quickly when Jared first encounters an obstacle, and slow down as the shock is compressed. Such a response ensures the shock with compress quickly at the beginning of the stroke, allowing the wheelchair to deal effectively with small bumps, but move slowly at the end of the stroke to avoid bottoming out.

Bond-Graph

Based on reference 1, a preliminary bond graph was created. The bond graph was modified to place the source of flow on the coupler, as the system input comes from bumps in the road that will be transmitted to the suspension system by means of the wheel shaft mounted at point E.

Unfortunately, the source of flow caused all states to be in derivative causality. Reference 1 had a second example for a four bar where additional bond graph components were added to cause all states to be in integral causality. While learning how to find the values of the added components, we read in reference 2 that the added components are “pads.” According to reference 2, the addition of springs and dampers in parallel to a bond graph can be used to simplify the state equations, and as long as the values for the added spring and

damper are sufficiently large, the effect on the dynamics of the system should be minimal. Thus the bond graph in Figure 6 was created.

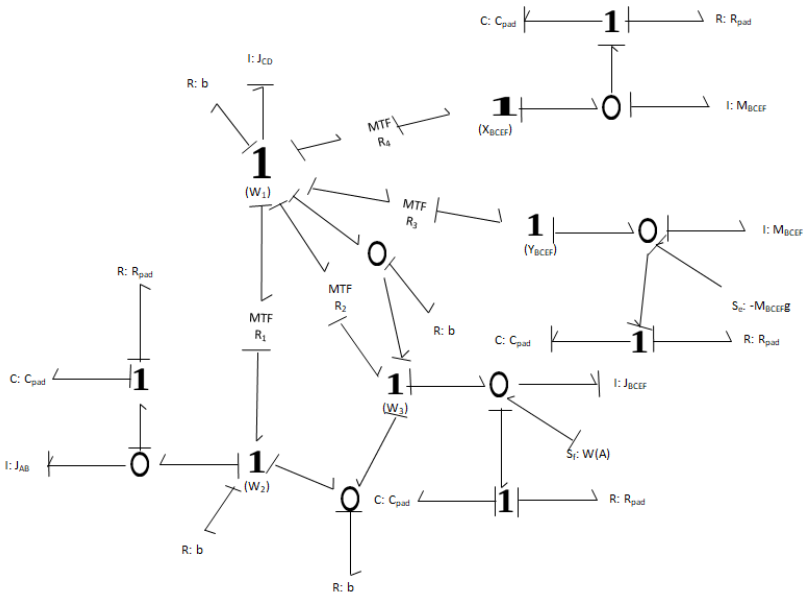

Figure 6: Second Iteration of our Bond-graph

As seen in Figure 6, all states were in integral causality as expected. At this step we began calculating all of the transformer moduli. The moduli can be calculated by first finding the equations to relate θ_1 to θ_2, θ_3, X_{bcef}, and Y_{bcef}. By then taking the derivative of each equation, the transformer moduli are found to relate ω_1 to ω_2, ω_3, Vx_{bcef}, and Vy_{bcef}. Figure 7 was used to calculate R_1 and R_2.

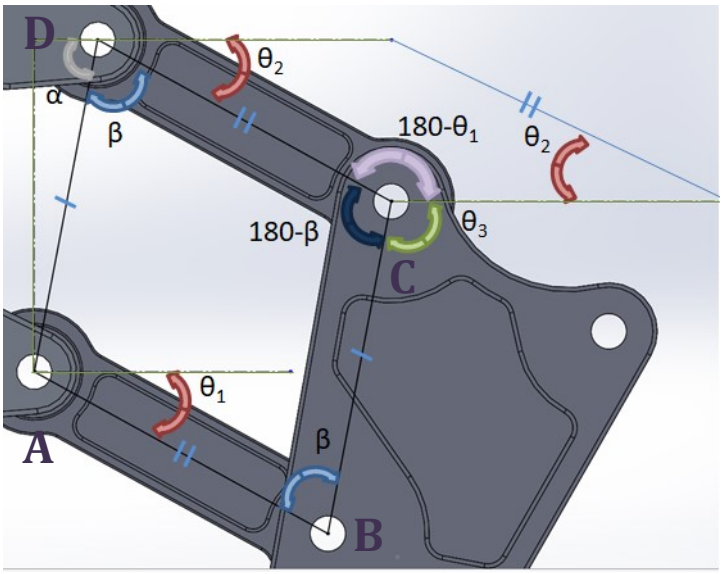

Figure 7: Solidworks Angle Modeling

In Figure 7, the green lines represent the X and Y axes respectively, while the blue tick marks denote parallel lines of equal length. That is to say, links AB and CD are parallel and equal, while AD and BC are also parallel and equal. As AB and CD are parallel, θ_1 is equal to θ_2, meaning ω_1 is equal to ω_2, as seen in equations 6.1 and 6.2.

$$\theta_1 = \theta_2 \quad (6.1)$$

$$\dot{\theta_1} = \dot{\theta_2} \quad (6.2)$$

As ω_1 is equal to ω_2, R_1 must be equal to 1, as shown in equations 6.3-6.5.

$$(1)\dot{\theta_1} = \dot{\theta_2} \quad (6.3)$$

$$R_1 * \dot{\theta_1} = \dot{\theta_2} \quad (6.4)$$

$$R_1 = 1 \quad (6.5)$$

As R_1 is equal to 1, all inputs and outputs to the respective modulated transformer are equal, and thus the modulated transformer can be removed.

R_2 can then be calculated similarly, using the additional symbols α and β, where α represents the constant angle between the grounded link AD and the x axis, and β represents the angle between AD and CD. Using geometry to solve for β and θ_3 yields equations 7.1 and 7.2 respectively, which when simplified, yield equations 7.3 – 7.5.

$$\beta = 180 - (\theta_1 + \alpha) \quad (7.1)$$

$$\theta_3 = 360 - (180 - \theta_1 + 180 - \beta) \quad (7.2)$$

$$\theta_3 = \theta_1 + \beta \quad (7.3)$$

$$\theta_3 = \theta_1 + 180 - (\theta_1 + \alpha) \quad (7.4)$$

$$\theta_3 = 180 - \alpha \quad (7.5)$$

As both 180 and α are constants, taking the derivative of equation 7.5 shows ω_3 to be equal to 0, as seen in equation 7.6.

$$\dot{\theta_3} = 0 \quad (7.6)$$

As ω_3 is equal to 0, including a 1 junction for ω_3 is inappropriate, and the 1 junction, along with all connected bonds, can be omitted. This also allows the modulated transformer with modulus R_2 to be removed, as it is connected to a grounded junction.

Equation 7.6 proves link BCEF does not rotate, which means the linear velocity at any point on link BCEF will be the same. This allows the x and y components of the linear velocity to be found at joint B instead of the center of mass. First, the x and y position components for joint B were calculated using equations 8.1x and 8.1y.

$$X_B = AB * \cos(\theta_1) \quad (8.1x)$$

$$Y_B = AB * sin(\theta_1) \quad (8.1y)$$

Then, by taking the derivative of both sides, as done previously, R_3 and R_4 were found.

$$V_{XB} = -\dot{\theta_1} * AB * \sin(\theta_1) \quad (8.2x)$$

$$V_{YB} = \dot{\theta_1} * AB * \cos(\theta_1) \quad (8.2y)$$

$$V_{XB} = R_3 * \dot{\theta_1} \ \therefore \ R_3 = -AB * sin(\theta_1) \quad (8.3x)$$

$$V_{YB} = R_4 * \dot{\theta_1} \ \therefore \ R_4 = AB * cos(\theta_1) \quad (8.3y)$$

By implementing the transformer simplifications previously detailed, and then simplifying flow through junctions, the bond graph in Figure 8 was derived. Unfortunately, when removing the 1 junction for W_3, the source of flow was also removed. We realized, however, the input flow would be more accurately modeled as a linear input velocity applied to the coupler.

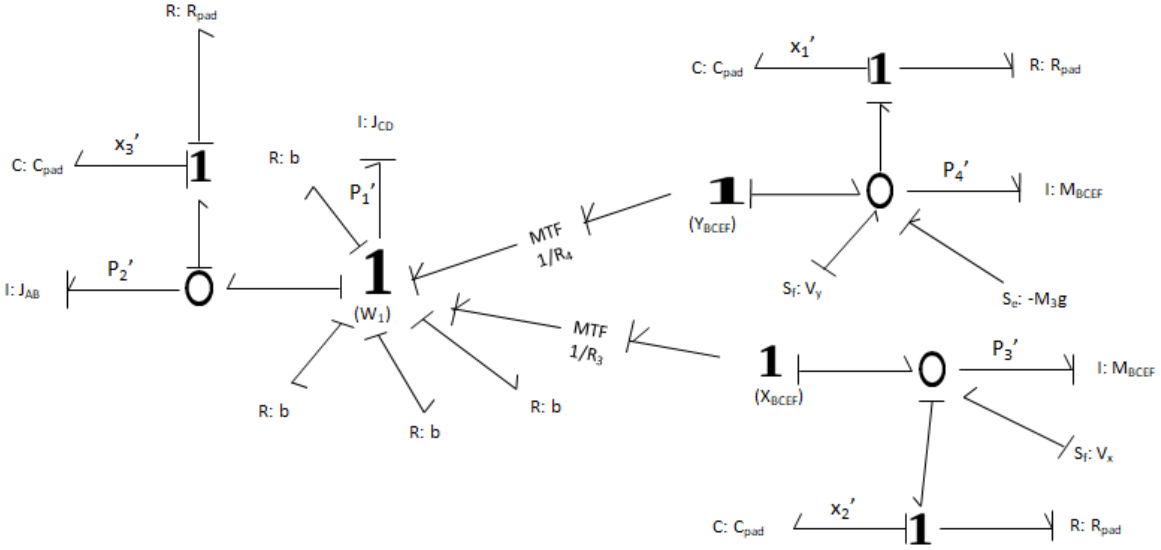

Figure 8: Simplified Padded Bond Graph with magnitude flow

During the simplification, we decided the transformer would be more accurately represented as pointing from the linear velocity to the angular velocity, as the input flow is a linear velocity. We used this iteration of the bond graph to calculate and plot a series of state equations. As will be further discussed in following sections, the matlab plots did not match the response we expected. To remedy this problem, we decided to remove the pads and observe the system response without them. To allow us to avoid having all terms in derivative causality as had happened prior, we discussed treating the input as a source of effort. We decided this would be appropriate as it would allow us to observe the reaction to large impacts where the force applied is more significant than the flow.

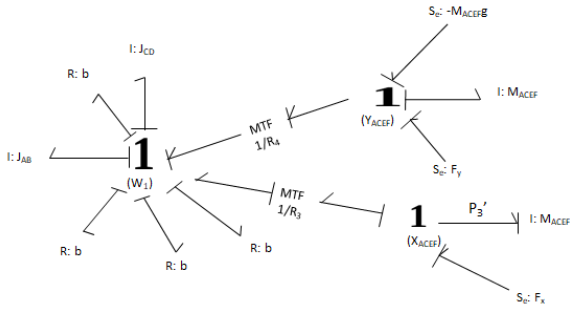

Figure 9: X Momentum Bond Graph

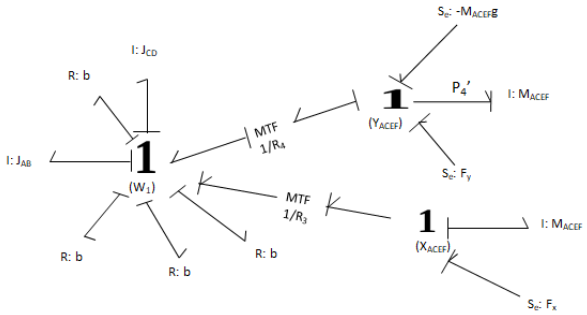

Figure 10: Y Momentum Bond Graph

As only one term can be in integral causality without the pads, the bond graphs in Figures 9 and 10 were created to allow observation of the x and y momentum. We did not create further bond graphs to include the other terms as we are primarily concerned with the behavior of the coupler.

State Equations

After completing the bond graphs and assigning causality, the bonds were labeled and we were assigned values to each bond. The resulting labeled bond graphs are shown above in Figures 9 and 10. Figure 8 yielded five state equations that appeared as follows.

$$\dot{X_1} = \frac{m_{bcef}g - C_{pad}X_1}{R_{pad}} \tag{9.1}$$

$$\dot{X_2} = V_x + R_3\left(\frac{h_1}{J_1}\right) - \frac{P_3}{m_3} \tag{10.1}$$

$$\dot{X_3} = \frac{h_1}{J_1} - \frac{h_2}{J_2} \tag{11.1}$$

$$\dot{P_3} = X_2C_{pad} + R_{pad}(V_x + R_3\left(\frac{h_1}{J_1}\right) - \frac{P_3}{m_3} \tag{12.1}$$

$$\dot{P_4} = m_3g \tag{13.1}$$

$$\dot{h_1} = R_3\left(X_2C_{pad} + R_{pad}\left(V_x + R_3\left(\frac{h_1}{J_1}\right) - \frac{P_3}{m_3}\right)\right) + R_4m_3g - \frac{4bh_1}{J_1} - \left(X_3C_{pad} + R_{pad}\left(\frac{h_1}{J_1} - \frac{h_2}{J_2}\right)\right) \tag{14.1}$$

$$\dot{h_2} = C_{pad}X_3 + R_{pad}\left(\frac{h_1}{J_1} - \frac{h_2}{J_2}\right) \tag{15.1}$$

These equations were inserted into Matlab, using the I and M values from Table 3, and tuned values for C_{pad} and R_{pad}. The bearing resistance was found using the following equation.

$$D = \frac{\pi\mu d^3 L}{4h} \tag{16.1}$$

Where d is the diameter of the shaft, L is the thickness of the bearing, and h is the thickness of the layer of grease. By measuring these values, and using the grease material properties in reference 3 for a common grease, the following damping value was calculated.

$$D = \frac{\pi(0.0595) * 0.44^3 * 0.27}{4\left(\frac{.87 - .44}{2}\right)} = 0.001\ (\text{lb} * \text{in} * \text{s}) \tag{16.2}$$

Such a method is adequate, as by assuming perfect machining in the sealed ball bearings, the resistance would come strictly from the viscous shear of the grease. After attempting to tune the values for C_{pad} and R_{pad}, the most realistic response was found by setting both values to 0. The state equation response with these tuned values is shown in Figure 11.

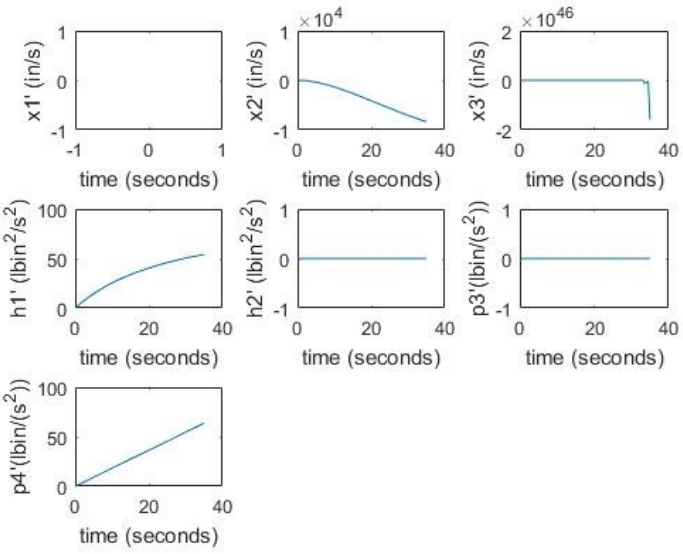

Figure 11: Matlab responses to State Equations

Even after tuning, the plots did not match the expected response, with the x momentum being equal only to zero. Consequently, the bond graph in Figures 9 and 10 was created by removing the pads. The single integral states yielded equations 17.6 and 18.6.

$$\dot{P}_3 = F_X - \frac{1}{R_3}\left(4b\omega_1 + \frac{d}{dt}(J_1\omega_1) + \frac{d}{dt}(J_2\omega_1) - \left(F_Y + m_3 g - \frac{d}{dt}(m_s Y_3)\right)R_4\right) \tag{17.1}$$

$$\frac{d}{dt}(J_1\omega_1) \therefore J_1\frac{d}{dt}\left(\frac{P_3}{m_3 R_3}\right) \therefore \frac{J_1\dot{P}_3}{m_3 R_3} \tag{17.2}$$

$$\frac{d}{dt}(J_2\omega_1) \therefore J_2\frac{d}{dt}\left(\frac{P_3}{m_3 R_3}\right) \therefore \frac{J_2\dot{P}_3}{m_3 R_3} \tag{17.3}$$

$$\frac{d}{dt}(m_3 Y_3) \therefore m_3\frac{d}{dt}\left(\frac{R_4 P_3}{m_3 R_3}\right) \therefore \frac{R_4\dot{P}_3}{R_3} \tag{17.4}$$

$$\dot{P}_3 = F_X - \frac{1}{R_3}(4b\omega_1 + \frac{J_1}{m_3}\left(\frac{1}{R_3}\right)\dot{P}_3 + \frac{J_2}{m_3}\left(\frac{1}{R_3}\right)\dot{P}_3 - \left(F_Y + m_3 g - \left(\frac{R_4}{R_3}\right)\dot{P}_3\right)R_4 \tag{17.5}$$

$$\dot{P}_3 = \frac{R_3 m_3\left(R_3 F_X - 4b\omega_1 + R_4 F_y + R_4 m_3 g\right)}{R_3^2 m_3 + R_4^2 m_3 + J_1 + J_2} \tag{17.6}$$

$$\dot{P}_4 = F_Y + m_3 g - \frac{1}{R_4}(4b\omega_1 + \frac{d}{dt}(J_1\omega_1) + \frac{d}{dt}(J_2\omega_1) - \left(F_X - \frac{d}{dt}(m_s X_3)\right)R_3 \tag{18.1}$$

$$\frac{d}{dt}(J_1\omega_1) \therefore J_1\frac{d}{dt}\left(\frac{P_4}{m_3 R_4}\right) \therefore \frac{J_1\dot{P}_4}{m_3 R_4} \tag{18.2}$$

$$\frac{d}{dt}(J_2\omega_1) \therefore J_2\frac{d}{dt}\left(\frac{P_4}{m_3 R_4}\right) \therefore \frac{J_2\dot{P}_4}{m_3 R_4} \tag{18.3}$$

$$\frac{d}{dt}(m_3 Y_3) \therefore m_3\frac{d}{dt}\left(\frac{R_3 P_4}{m_3 R_4}\right) \therefore \frac{R_3\dot{P}_4}{R_4} \tag{18.4}$$

$$\dot{P}_4 = F_Y + m_3 g - \frac{4b\omega_1}{R_4} - \frac{J_1}{m_3}\left(\frac{1}{R_4^2}\right)\dot{P}_4 - \frac{J_2}{m_3}\left(\frac{1}{R_4^2}\right)\dot{P}_4 - \frac{F_X R_3}{R_4} - \left(\frac{R_4^2}{R_3^2}\right)\dot{P}_4 \tag{18.5}$$

$$\dot{P}_4 = \frac{R_4 m_3(R_4 F_Y + R_4 m_3 g - 4b\omega_1 + R_3 F_x)}{R_3^2 m_3 + R_4^2 m_3 + J_1 + J_2} \tag{18.6}$$

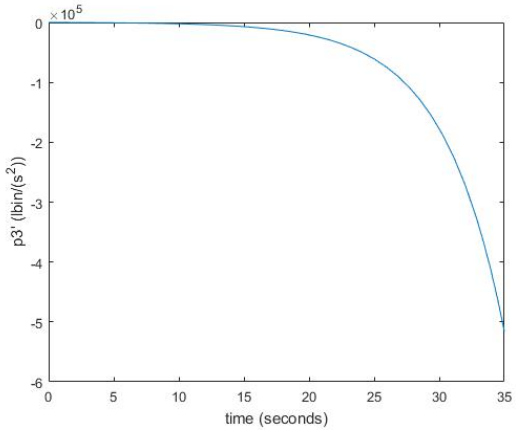

Figure 12: P3 State Equation Plot

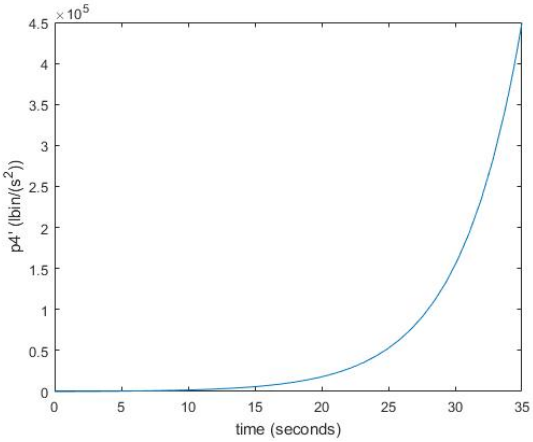

Figure 13: P4 State Equation Plot

Figures 12 and 13 show the response of the X and Y magnitude components respectively. As expected, the x and y magnitudes at any given time are roughly opposite. However, the magnitudes of each plot are much larger than expected.

Discussion

Being able to generate plots for the dynamic force analysis and state equations was useful as they allowed us to evaluate our hypothesis of how the physical system will work. A future iteration could account for the rear suspension, to provide a better representation of how the entire wheelchair would behave. Inputs of varying forces should also be considered to see specifically how the system responds to sharp impacts, and gradually increasing forces. To further increase accuracy, we could contact the vendor of the bearings to determine the specific type of grease used to have a better representation of the bearing damping.

References

- *Intelligent Mechatronic Systems*. [Online]. Available: https://link.springer.com.ezproxy.wpi.edu/book/10.1007%2F978-1-4471-4628-5. [Accessed: 1-Mar-2018].
- *Independence Control of Space Robots Using Passive Degrees of Freedom in Controller Domain.* [Online]. Available: http://au4sb9ax7m.search.serialssolutions.com/?ctx_ver=Z39.88-2004&ctx_enc=info%3Aofi%2Fenc%3AUTF-8&rfr_id=info%3Asid%2Fsummon.serialssolutions.com&rft_val_fmt=info%3Aofi%2Ffmt%3Akev%3Amtx%3Ajournal&rft.genre=article&rft.atitle=Impedance+Control+of+Space+Robots+Using+Passive+Degrees+of+Freedom+in+Controller+Domain&rft.jtitle=Journal+of+Dynamic+Systems%2C+Measurement%2C+and+Control&rft.au=Pathak%2C+Pushparaj+Mani&rft.au=Mukherjee%2C+Amalendu&rft.au=Dasgupta%2C+Anirvan&rft.date=2005&rft.issn=0022-0434&rft.eissn=1528-9028&rft.volume=127&rft.issue=4&rft.spage=564&rft_id=info:doi/10.1115%2F1.2098894&rft.externalDBID=n%2Fa&rft.externalDocID=10_1115_1_2098894&paramdict=en-US. [Accessed: 1-Mar-2018]
- *Viscopedia*. [Online]. Available: http://www.viscopedia.com/viscosity-tables/substances/gear-oil/. [Accessed: 1-Mar-2018].